A Comparative Study of RCS Computation Codes

Chia Tse Tong (ctsetong@dso.org.sg)*, **Ang** Teng Wah,
Lim Kheng Hwee, **Ou** Sheng Chye Philip, **Yar** Kar Heng
DSO National Laboratories
20 Science Park Dr, Singapore 118230

David **Rowse**, Matthew **Amos**, Alan **Keen**, Neil **Pegg**, Andrew **Thain**
Advanced Technology Centre, BAE Systems Plc
Bristol BS34 7QW United Kingdom

1. INTRODUCTION

This paper reports the results of an ongoing study between BAE Systems, U.K., and DSO National Laboratories, Singapore, into the accuracy, performance and capabilities of computational electromagnetics (CEM) codes. For the purpose of this paper, we will report two of the selected test cases, a re-sized NASA almond, a generic missile and the COBRA inlet.

2. TEST CASES

The two test objects are shown in Figure 1. The first test object is a (fictitious) generic missile. It provides a test problem for benchmarking the performance of CEM codes on geometries containing "real world" deficiencies, such as thin bodies and sharp corners. The long missile has a trapezoidal body cross-section with planform sweep angles of 55°. A boat-tail at the rear obscures the exhaust. The intake, not shown for RCS calculation purposes, is assumed to be conformal. The nose tip is sharp to avoid spherical scatter. The overall length, width and height of the missile are 5.9m, 2.3m and 0.7m, respectively.

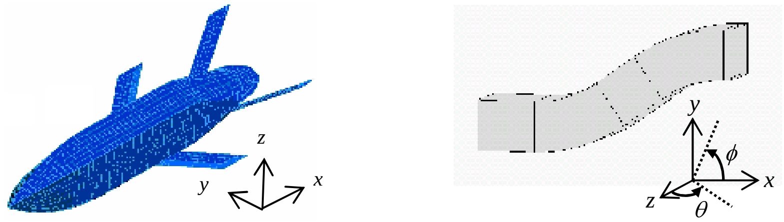

(a) **(b)**
Figure 1: Test cases: (a) generic missile, (b) COBRA inlet.

The second test object is the COBRA inlet designed and manufactured by EADS Aerospatiale Matra Missiles for the JINA 98 workshop. The COBRA inlet is an S-bend rectangular metallic cavity constructed from five continuous segments. The first segment is a straight rectangular cavity of length 10mm. Following this segment is a 35° circular bend of radius 186mm. The third segment is another straight section of length 80mm, followed by another 35° circular bend of radius of 186mm. The final straight segment of the cavity is 100mm long and is terminated by a PEC plate. The cross section of the cavity is 84mm × 110mm.

Report Documentation Page

Form Approved
OMB No. 0704-0188

1. REPORT DATE **01 JAN 2005**	2. REPORT TYPE **N/A**	3. DATES COVERED **-**

4. TITLE AND SUBTITLE **A Comparative Study of RCS Computation Codes**	5a. CONTRACT NUMBER 5b. GRANT NUMBER 5c. PROGRAM ELEMENT NUMBER
6. AUTHOR(S)	5d. PROJECT NUMBER 5e. TASK NUMBER 5f. WORK UNIT NUMBER
7. PERFORMING ORGANIZATION NAME(S) AND ADDRESS(ES) **DSO National Laboratories 20 Science Park Dr, Singapore 118230**	8. PERFORMING ORGANIZATION REPORT NUMBER
9. SPONSORING/MONITORING AGENCY NAME(S) AND ADDRESS(ES)	10. SPONSOR/MONITOR'S ACRONYM(S) 11. SPONSOR/MONITOR'S REPORT NUMBER(S)

12. DISTRIBUTION/AVAILABILITY STATEMENT
Approved for public release, distribution unlimited

13. SUPPLEMENTARY NOTES
See also ADM001846, Applied Computational Electromagnetics Society 2005 Journal, Newsletter, and Conference., The original document contains color images.

14. ABSTRACT

15. SUBJECT TERMS

16. SECURITY CLASSIFICATION OF:			17. LIMITATION OF ABSTRACT	18. NUMBER OF PAGES	19a. NAME OF RESPONSIBLE PERSON
a. REPORT **unclassified**	b. ABSTRACT **unclassified**	c. THIS PAGE **unclassified**	**UU**	**4**	

Standard Form 298 (Rev. 8-98)
Prescribed by ANSI Std Z39-18

3. CEM CODES USED

The CEM codes used are indicated in Table 1. As the methods used are generally well-known, no description will be provided here. The computational parameters for obtaining the monostatic RCS for the test objects are given in Table 2.

Table 1: Codes used in investigation.

Code	Computational method
FM3D	Multi-Level Fast Multi-Pole Algorithm
FEBI	Finite Element Boundary Integral Method
PO-PTD	Physical Optics with PTD
MITRE	Physical Optics
IPO-PO	Hybrid Iterative PO with Physical Optics

Table 2: Definition of test cases.

Test Case	Code	Frequency	Polarisation	Mesh	Theta	Phi	Δϕ
Generic Missile M-1	FM3D FEBI PO-PTD MITRE	1 GHz	VV, HH	λ/15 λ/15 Biquad Biquad	90°	0° – 180°	0.4°
Generic Missile M-2	PO-PTD MITRE	10 GHz	VV, HH	Biquad	90°	0° – 180°	0.4°
COBRA inlet	FM3D FEBI IPO-PO	10 GHz	θθ, ϕϕ	λ/15 λ/6 0.2λ	90°	-90° – 90°	0.5°

4. RESULTS & DISCUSSION

Figure 2 shows the predicted RCS of the missile at 1GHz from FM3D and FEBI using a λ/15 mesh, and from PO-PTD and MITRE using a biquadratic mesh. It can be seen from the figure that the results of the FM3D and FEBI codes agree very closely, with slight differences toward the rear (0°) and the nose (180°) for the horizontal and vertical polarizations, respectively.

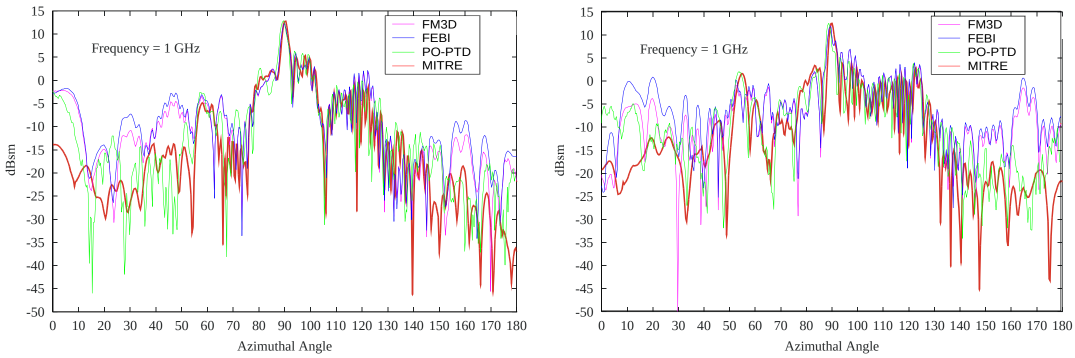

Figure 2: Monostatic RCS of generic missile at 1GHz (Test Case M-1). (a) VV-pol; (b) HH-pol.

In terms of the major features of RCS peaks and lobes, there is overall good agreement between the MITRE and PO-PTD results in Figure 2. The obvious disagreements between the two results are near the rear and frontal aspects. The disagreement is due

likely to the lack of multiple scattering and/or self-shadowing effects in MITRE. The same comments apply to Figure 3 for the 10GHz case.

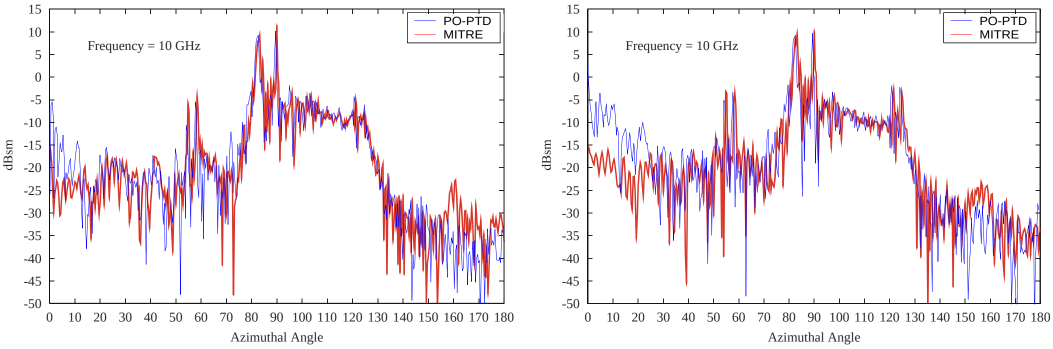

Figure 3: Monostatic RCS of generic missile at 10GHz (Test Case M-2). (a) VV-pol; (b) HH-pol.

Comparing the results from the "low frequency" and "high frequency" codes in Figure 2, there is fairly good agreement between their results for the angular sector from about 50° to 150°. Therefore, we can conclude that physical optics field dominates in this sector. However, the two sets of results do not match well in the frontal and rear sectors. In fact, PO tends to underestimate the RCS in these sectors. Therefore, there are other wave phenomena, such as travelling waves and higher order diffraction, that gives rise to the larger RCS obtained by the low frequency codes. In particular, the peaks observed at close to 10° and 170°, especially for the horizontal polarization, are most likely due to travelling waves reflecting back in the incident direction. The maximum backscatter direction due to travelling waves is given by $49.35(\lambda/L)^{½}$ [1] where L is the length along which the waves travel on a long smooth structure. Using the length of the platform (about 5.9m) for L, the backscatter direction (measured from the surface of the structure) is about 11°, which corresponds to the two peaks observed around 10° and 170°.

Figure 4 shows the predicted RCS of the COBRA inlet at 10GHz using FM3D, FEBI and IPO-PO. The RCS is the sum of the external scattering and the internal cavity scattering. There is good agreement between the results obtained by FM3D and FEBI. The agreement between these results and the IPO-PO results is good over most of the angular range, except for the angular range $10° < \phi < 70°$, where there are significant differences. There are two possible causes. Firstly, the IPO formulation suffers from inaccuracy when the aperture of the inlet is smaller than 3λ (the COBRA inlet aperture is 2.8λ x 3.67λ at 10GHz). Secondly, the creeping waves phenomenon generated at the lower wall of the S-bend inlet is not taken into account in the IPO formulation.

Table 3 and Table 4 provide a summary of the runtime and memory usage for the different codes used to obtain the results for the generic missile and the COBRA inlet, respectively.

Table 3: Computing resources used for generic missile at 1GHz.

Code	CPU time (s)	Memory (Mb)	Machine Type
FEBI	147,554	136	3.2GHz PC, 4GB RAM
FM3D	78,760	2,269	1GHz Alpha EV6
PO-PTD	415	768	800MHz PC, 768 RAM
MITRE	200	13	2.8GHz PC

Table 4: Simulation Time and Memory Usage for Cobra.

Codes	Simulation time	Memory usage	Machine Type
FM3D	939,925 sec (457,000 sec - θθ) (482,925 sec - ϕϕ)	8.3 GB	AMD Linux cluster using 11 x 1.4GHz CPU
FEBI	2,100	710 MB	Intel Xeon 3.2GHz
IPO-PO	89,277 sec	21.5 MB	1.4GHz PC

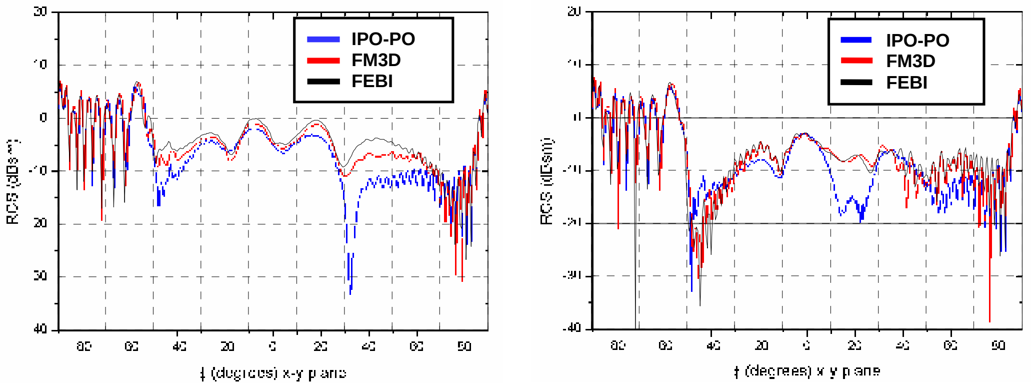

Figure 4: Monostatic RCS of COBRA inlet at 10GHz. (a) θθ - pol; (b) ϕϕ - pol.

5. SUMMARY

We have presented and compared the predicted RCS of two test targets obtained via various CEM codes. The agreement between the codes is good in general although differences exist even for codes using the same computational method. Some of the differences are due to limitations inherent in the computational method.

Acknowledgement

This work was funded by the Defence Science & Technology Agency, Singapore and BAE Systems plc.

References

[1] David Jenn, Radar and Laser Cross Section Engineering, 1995, AIAA, pg. 69.